Title	Discussion of "Statistics of model factors in reliability-based design of axially loaded driven piles in sand"
Author(s)	Flynn, Kevin N.; McCabe, Bryan A.
Publication Date	2018-11-22
Publication Information	Flynn, Kevin N., & McCabe, Bryan A. (2018). Discussion of "Statistics of model factors in reliability-based design of axially loaded driven piles in sand". Canadian Geotechnical Journal, 56(1), 144-147. doi: 10.1139/cgj-2018-0217
Publisher	NRC Research Press
Link to publisher's version	https://dx.doi.org/10.1139/cgj-2018-0217
Item record	http://hdl.handle.net/10379/14767
DOI	http://dx.doi.org/10.1139/cgj-2018-0217

Please cite as:

Flynn, K.N. and McCabe, B.A. (2019) Discussion of "Statistics of Model Factors in Reliability-Based Design of Axially Loaded Displacement Piles in Sand" by C. Tang and K.-K. Phoon, *Canadian Geotechnical Journal*, Vol. 56, No. 1, pp. 144-147.

Authors' response available at:

Tang, C. and Phoon, K.-K. (2019) Reply to the discussion by Flynn and McCabe on "Statistics of Model Factors in Reliability-Based Design of Axially Loaded Displacement Piles in Sand", *Canadian Geotechnical Journal*, 56(1): 148-152.

Discussion of "Statistics of Model Factors in Reliability-Based Design of Axially Loaded Displacement Piles in Sand" by C. Tang and K.-K. Phoon

Kevin N. Flynn[1] & Bryan A. McCabe[2*]

[1]Senior Geotechnical Engineer, AGL Consulting, Sandyford, Dublin 18, Ireland

[2]Senior Lecturer, College of Engineering & Informatics, National University of Ireland Galway, Ireland

*Corresponding author: bryan.mccabe@nuigalway.ie

Tang and Phoon (2018) have presented a comprehensive statistical treatment of model factors for axially-loaded displacement piles in sand at both ultimate limit state (ULS) and serviceability limit state (SLS). The results of this study make a significant contribution to reliability-based design of deep foundations.

In order to derive their model factors, the authors collated high-quality compression and tension load test data for a range of displacement pile types founded in sand, using (i) the ZHU-ICL (Yang et al. 2015, 2017) database, (ii) the FHWA DFLTD (Abu-Hejleh et al. 2015) database, and (iii) selected compression load test data for driven cast-in-situ (DCIS) piles from a database published by Flynn (2014). DCIS piles classify as large displacement piles as a steel tube (with a sacrificial base plate) is driven as the first stage of the pile construction process. The authors' justification for including DCIS piles in the study is the case history evidence (Flynn et al. 2013, 2014; Flynn and McCabe 2016) that their shaft and base resistances at ULS are comparable to those for traditional closed-ended preformed displacement piles such as precast concrete or steel piles.

For ULS model factors, the authors calculated the total pile resistance $R_{u,c}$ from Cone Penetration Test (CPT) data using the ICP-05 (Jardine et al. 2005) and UWA-05 (Lehane et al. 2005) methods, enabling the ratio of measured total resistance ($R_{u,m}$) to $R_{u,c}$ to be obtained for each pile. The mean values of $R_{u,m}/R_{u,c}$ and the corresponding coefficients of variation (COV) derived for both methods are in keeping with previous such assessments by Jardine et al. (2005), Lehane et al. (2005) and Flynn et al. (2014) for each of the displacement pile sub-categories in the database.

The assessment of SLS model factors required the authors to fit hyperbolic curves to a total of 117 No. normalized pile load-displacement curves in the database using the following equation (Phoon et al., 2006):

$$\frac{Q}{Q_{ref}} = \frac{s}{a+bs} \qquad \text{Equation D1}$$

where Q is the applied load at the pile head, Q_{ref} is the interpreted pile resistance, s is the pile head displacement and a and b are the hyperbolic curve fitting parameters. The authors have chosen the L_2 resistance (Q_{L2}) proposed by Hirany and Kulhawy (1989) as their Q_{ref} value. The relationship between *a* and *b* for the closed-ended piles was examined using a scatter plot to determine the degree of correlation for use in the statistical simulations for deriving the SLS model factors. The authors did not distinguish between the various displacement pile types (i.e. preformed closed-ended and DCIS piles) when examining the scatter plot. This exercise has been carried out by the discussers for the preformed closed-ended piles (CEP) and DCIS piles under compression loading and is illustrated in Figure D1. While a significant degree of scatter is evident (due to variations in pile dimensions, ground conditions etc.), there is no obvious difference in *a* and *b* values for the CEP and DCIS piles.

The discussers believe that normalization of the pile load test data by the L_2 value has concealed important differences in the load-displacement behavior of DCIS and preformed driven displacement piles observed in load tests, and therefore have performed a similar statistical study based on the use of the slope tangent resistance (Q_{ST}) in Equation D1. While the slope tangent resistance is considered overly-conservative as a definition of ultimate pile capacity (NeSmith and Siegel, 2009), it has been shown to be acceptable for the purposes of assessing variations in load-displacement behavior for cast-in-situ pile types, based on data presented by Chen and Kulhawy (2010).

The discussers' database comprises (i) 18 No. DCIS pile load tests: 7 No. instrumented tests carried out by Flynn (2014), as well as 6 No. tests reported in the literature, and (ii) load test data for 27 No. closed-ended preformed displacement piles (i.e. precast concrete or steel) from the UWA-05 database. Table D1 presents a summary of the DCIS database, while the displacement piles from the UWA-05 database are summarized in Table D2; each table provides details of pile type, dimensions, interpreted capacities and normalized hyperbolic parameters. A plot of Q_{ST} against Q_{L2} for the DCIS and closed-ended preformed displacement piles (Figure D2) clearly differentiates between two pile types, with mean ratios of Q_{ST}/Q_{L2} = 0.72 for the DCIS piles and Q_{ST}/Q_{L2} = 0.91 for the closed-ended preformed displacement piles implying distinctly different load-displacement responses. Significantly, the mean Q_{ST}/Q_{L2} ratio for the DCIS piles is similar to that reported by Chen and Kulhawy (2010) for auger cast-in-place piles (ACIP). This may be attributed to the absence of driving-related residual loads in both cases; in the case of DCIS piles, these residual loads are eliminated upon in situ concreting once the tube is withdrawn (Flynn 2014, Flynn and McCabe 2016).

Figure D3 presents the scatter plot of the normalized curve fitting parameters for the DCIS and preformed displacement piles using the slope tangent resistance Q_{ST}. Unlike the scatter plot in Figure D1 (based on the L_2 resistance), a discernible difference in parameters is apparent for the two pile types, with mean parameters for DCIS and closed-ended preformed displacement piles of a = 5.81mm, b = 0.51 and a = 2.95mm, b = 0.77, respectively. As noted by the authors, a large a value implies a small initial slope of the load-settlement curve, resulting in a slowly decaying (i.e. ductile) load-displacement response. As such, the above parameters would imply that the mean shape of the DCIS load-displacement curve is more ductile than the closed-ended preformed displacement piles. A number of DCIS data points in Figure D3 plot in close proximity to the preformed pile dataset. Inspection of these data has indicated that the contribution of the shaft resistance to the total pile resistance during loading was minimal for these piles and hence the pile behavior (and shape of the load-displacement curve) was dominated by the base resistance. As noted by Flynn (2014), Flynn et al. (2014) and Flynn and McCabe (2016), the base resistance of DCIS piles is nearly identical to closed-ended preformed driven piles. Hence, prediction of the load-displacement behavior of DCIS piles is further complicated by the respective contribution of the shaft and base resistances during loading.

In conclusion, the results of the Tang and Phoon (2018) study would appear to suggest that the SLS behavior of DCIS piles is similar to closed-ended preformed displacement piles under axial compression loading. This outcome is not in keeping with the discussers' experience of the measured load-displacement response of DCIS piles, which tends to exhibit a more ductile response during loading when compared to closed-ended preformed displacement piles, primarily due to the in situ concreting (once the tube is withdrawn), which eliminates the driving-induced residual loads, and leads to enhanced interface friction properties along the pile shaft. The hyperbolic curve fitting parameters of normalized load-displacement curves for DCIS piles is strongly dependent on the failure criterion chosen, and proportion of load carried by the pile shaft. Therefore, the inclusion of DCIS pile test data when deriving overall SLS model factors for displacement piles in sand is not advised.

References

Abu-Hejleh, N.M., Abu-Farsakh, M., Suleiman, M.T., and Tsai, C. 2015. Development and use of high-quality databases of deep foundation load tests. Transportation Research Record: Journal of the Transportation Research Board, No. 2511: 27-36.

Altaee, A., Fellenius, B.H. and Evgin, E. 1992. Axial load transfer for piles in sand. I. Tests on an instrumented precast pile. Canadian Geotechnical Journal, 29(1): 11-20.

Appendino, M. 1981. Interpretation of axial load tests on long piles. *In* Proceedings of the 10th International Conference on Soil Mechanics and Foundation Engineering, Stockholm, 15-19 June 1981. A.A. Balkema, Rotterdam, the Netherlands, pp. 592-598.

Axelsson, G. 2000. Long term setup of driven piles in sand. Ph.D. thesis, Royal Institute of Technology, Stockholm, Sweden.

Beringen, F.L., Windle, D. and Van Hooydonk, W.R. 1979. Results of loading tests on driven piles in sand. *In* Proceedings of the Conference on Recent Development in the Design and Construction of Piles, ICE, London, 21-22 March 1979, Institution of Civil Engineers, London, UK, pp. 213-225.

Briaud, J.-L., Moore, B.H. and Mitchell, G.B. 1989a. Analysis of pile load tests at Lock and Dam 26. *In* Foundation engineering: Current principles and practices, Evanston, Ill., American Society of Civil Engineers, Reston, VA., pp. 925-942.

Briaud, J.-L., Tucker, L.M. and Ng, E. 1989b. Axially loaded 5 pile group and single pile in sand. *In* Proceedings of the 12th International Conference on Soil Mechanics and Foundation Engineering, pp. 1121-1124.

Chen, J.-R. and Kulhawy, F.H. 2010. Axial load-displacement behavior of augered cast-in place piles and pressure-injected footings. *In* GeoFlorida 2010: Advances in Analysis, Modeling & Design (GSP 199), American Society of Civil Engineers, Reston, VA., pp. 523-1532.

De Beer, E., Lousberg, D. De Jonghe, A., Carpentier, R. and Wallays, M. 1979. Analysis of the results of loading tests performed on displacement piles of different types and sizes penetrating a relatively small depth into a very dense layer. *In* Proceedings of the Conference on Recent Development in the Design and Construction of Piles, 21-22 March 1979. Institution of Civil Engineers, London, UK, pp. 199-211.

Evers, G., Hass, G., Frossard, A., Bustamante, M., Borel, S. and Skinner, H. 2003. Comparative performances of continuous flight auger and driven cast in place piles in sands. *In* Proceedings of the 4th International Geotechnical Seminar on Deep Foundations on Bored and Auger Piles, Ghent, Belgium, pp. 137–144.

Flynn, K.N. 2014. Experimental investigations of driven cast-in-situ piles. Ph.D. thesis. College of Engineering and Informatics, National University of Ireland, Galway, Ireland.

Flynn, K.N., and McCabe, B.A. 2016. Shaft resistance of driven cast-in-situ piles in sand. Canadian Geotechnical Journal, 53(1): 45-59.

Flynn, K.N., McCabe, B.A. and Egan, D. 2013. Axial load behavior of a driven cast in situ pile in sand. In: Proceedings of the 7th International Conference on Case Histories in Geotechnical Engineering, Chicago. Paper No. 2.49.

Flynn, K.N., McCabe, B.A., and Egan, D. 2014. Driven cast-in-situ piles in granular soil: application of CPT methods to pile capacity estimation. *In* Proceedings of the 3rd International Symposium on Penetration Testing, Las Vegas, USA.

Gregersen, O.S., Aas, G. and Di Biagio, E. 1973. Load tests on friction piles in loose sand. *In* Proceedings of the 8th International Conference on Soil Mechanics and Foundation Engineering, Moscow. Vol. 2, pp. 109-117.

Hirany, A., and Kulhawy, F. H. 1989. Interpretation of load test on drilled shafts 1: Axial compression. *In* Foundation engineering: Current principles & practices (GSP 22), American Society of Civil Engineers, Reston, VA., pp. 1132-1149.

Jardine, R.J., Chow, F.C., Overy, R., and Standing, J. R. 2005. ICP design methods for driven piles in sands and clays. Thomas Telford, London.

Lehane, B.M., Schneider, J.A., and Xu, X. 2005. The UWA-05 method for prediction of axial capacity of driven piles in sand. *In* Proceedings of the International Symposium on Frontiers in Offshore Geomechanics ISFOG. Taylor & Francis, London. pp. 683-689.

NeSmith, V.M., and Siegel, T.C. 2009. Shortcomings of the Davisson offset limit applied to axial compressive load tests on cast-in-place piles. *In* Proceedings of 2009 International Foundation Congress and Equipment Expo, Orlando, Florida, GSP No. 185, American Society of Civil Engineers, Reston, VA., pp. 568-574.

Nevels, J.B.J. and Snethen, D.R. 1994. Comparison of settlement predictions for single piles in sand based on penetration test results. *In* Proceedings of the Conference on Vertical and Horizontal Deformations of Foundations and Embankments, American Society of Civil Engineers, Reston, VA.,, pp. 1028–1038.

Paik, K., Salgado, R., Lee, J.H. and Kim, B. 2003. Behavior of open- and closed-ended piles driven into sands. Journal of Geotechnical and Geoenvironmental Engineering. 129(4): 296–306.

Phoon, K.K., Chen, J.R., and Kulhawy, F.H. 2006. Characterization of model uncertainties for augered cast-in-place (ACIP) piles under axial compression. *In* Foundation Analysis & Design: Innovative Methods (GSP 153), Reston, pp. 82-89.

Suckling, T. 2003. Driven cast insitu piles - the CPT and SPT - two case studies. Ground Engineering. 36(10): 28–32.

Titi, H.H. and Abu-Farsakh, M.Y. 1999. Evaluation of bearing capacity of piles from cone penetration test data. Louisiana Transportation Research Center, Baton Rouge, LA.

Vesic, A.S. 1970. Tests on instrumented piles, Ogeechee River site. Journal of the Soil Mechanics and Foundations Division. Proceedings of the American Society of Civil Engineers, 96(SM2): 561-584.

Yang, Z.X., Jardine, R.J., Guo, W.B., and Chow, F. 2015. A comprehensive database of tests on axially loaded piles driven in sands. Zhejiang University Press & Elsevier.

Yang, Z.X., Guo, W.B., Jardine, R.J., and Chow, F. 2017. Design method reliability assessment from an extended database of axial load tests on piles driven in sand. Canadian Geotechnical Journal, 54 (1): 59-74.

Yen, T.L., Chin, C.T. and Wang, R.F. 1989. Interpretation of instrumented driven steel pipe piles. *In* Proceedings of Congress of Foundation Engineering, Current Principles and Practices, Evanston, Ill., 25-29 June 1989. American Society of Civil Engineers, New York. pp. 1293-1308.

Table D1. Database of driven cast-in-situ piles

Test site location	Pile No.	Type	Material	Shape	Length (m)	Diameter (m)	Q_{ST} (kN)	Q_{L2} (kN)	a (mm)	b	Reference
Avonmouth	P3792	DCIS	Concrete	Circular	10.5	0.380	602	829	5.32	0.45	Flynn 2014
Avonmouth	TP1	DCIS	Concrete	Circular	8.8	0.380	592	1098	4.23	0.46	Flynn 2014
Dagenham	D1	DCIS	Concrete	Circular	7.7	0.380	1390	2347	7.12	0.38	Flynn 2014
Erith	E3	DCIS	Concrete	Circular	11.0	0.380	1489	1759	4.62	0.69	Flynn 2014
Ryton	R1	DCIS	Concrete	Circular	6.0	0.380	952	1442	4.09	0.48	Flynn 2014
Ryton	R2	DCIS	Concrete	Circular	7.0	0.380	1197	1401	4.62	0.63	Flynn 2014
Ryton	R3	DCIS	Concrete	Circular	5.5	0.380	1134	1951	6.04	0.36	Flynn 2014
Shotton	S1	DCIS	Concrete	Circular	5.75	0.380	1565	2152	7.67	0.51	Flynn 2014
Tilbury	T1	DCIS	Concrete	Circular	14.9	0.630	3929	5556	10.38	0.38	Flynn 2014
Dublin	TP1	DCIS	Concrete	Circular	15.6	0.430	2234	3997	7.20	0.31	Unpublished
Dublin	TP2	DCIS	Concrete	Circular	15.2	0.430	1959	3498	9.16	0.26	Unpublished
Le Havre	A4	DCIS	Concrete	Circular	10.5	0.430	1391	1600	3.63	0.73	Evers et al. 2003
Le Havre	C1	DCIS	Concrete	Circular	10.5	0.430	1534	1800	4.07	0.72	Evers et al. 2003
Gravesend	TP14	DCIS	Concrete	Circular	16.0	0.290	491	589	3.97	0.64	Suckling 2003
Ringsend	TP20	DCIS	Concrete	Circular	12.5	0.430	1735	2811	6.36	0.38	Suckling 2003
Kallo	K5	DCIS	Concrete	Circular	9.3	0.410	1387	1470	4.80	0.70	De Beer et al. 1979
Kallo	K6	DCIS	Concrete	Circular	11.4	0.410	3665	4130	5.09	0.74	De Beer et al. 1979

Table D2. Database of selected driven closed-ended displacement piles from the UWA-05 database

Test site location	Pile No.	Type	Material	Shape	Length (m)	Diameter (m)	Q_{ST} (kN)	Q_{L2} (kN)	a (mm)	b	Reference
Baghdad	P1	Closed-end	Concrete	Square	11.0	0.253	965	1002	1.19	0.87	Altaee et al. 1992
Baghdad	P2	Closed-end	Concrete	Square	15.0	0.253	1146	1503	1.43	0.67	Altaee et al. 1992
Cimarron River	P2	Closed-end	Concrete	Octagonal	19.5	0.610	2608	3125	3.23	0.72	Nevels and Snethen 1994
Drammen	A	Closed-end	Concrete	Circular	8.0	0.280	240	284	1.68	0.77	Gregersen et al. 1973
Drammen	D-A	Closed-end	Concrete	Circular	16.0	0.280	463	504	0.74	0.89	Gregersen et al. 1973
Drammen	E	Closed-end	Concrete	Circular	3.5	0.280	186	210	1.34	0.78	Gregersen et al. 1973
Drammen	E	Closed-end	Concrete	Circular	7.5	0.280	173	199	1.63	0.76	Gregersen et al. 1973
Drammen	E	Closed-end	Concrete	Circular	11.5	0.280	273	271	1.71	0.76	Gregersen et al. 1973
Drammen	E	Closed-end	Concrete	Circular	15.5	0.280	401	437	1.94	0.77	Gregersen et al. 1973
Drammen	E	Closed-end	Concrete	Circular	19.5	0.280	544	601	1.97	0.77	Gregersen et al. 1973
Drammen	E	Closed-end	Concrete	Circular	23.5	0.280	716	811	3.37	0.71	Gregersen et al. 1973
Fittja Straits	D	Closed-end	Concrete	Square	12.8	0.235	307	319	2.43	0.79	Axelsson 2000
Ogeechee River	H-2	Closed-end	Concrete	Square	15.2	0.406	2495	2587	3.15	0.86	Vesic 1970
Tickfaw River	TP2	Closed-end	Concrete	Square	25.9	0.610	3393	3376	1.88	0.93	Titi and Abu-Farsakh 1999
Cimarron River	P1	Closed-end	Steel	Circular	19.0	0.660	2608	3125	3.23	0.72	Nevels and Snethen 1994
Hoogzand	II	Closed-end	Steel	Circular	6.8	0.356	2652	2663	1.79	0.83	Beringen et al. 1979
Hsin Ta	TP4	Closed-end	Steel	Circular	34.2	0.610	4015	4122	5.06	0.79	Yen et al. 1989
Hunter’s Point	S	Closed-end	Steel	Circular	7.8	0.273	407	477	2.07	0.78	Briaud et al. 1989b
Lock & Dam 26	3-1	Closed-end	Steel	Circular	12.2	0.305	918	1108	2.72	0.67	Briaud et al. 1989a
Lock & Dam 26	3-4	Closed-end	Steel	Circular	14.4	0.356	849	876	3.80	0.65	Briaud et al. 1989a
Lock & Dam 26	3-7	Closed-end	Steel	Circular	14.6	0.406	1158	1550	2.93	0.62	Briaud et al. 1989a
Ogeechee River	H12	Closed-end	Steel	Circular	6.1	0.457	1854	2096	2.42	0.86	Vesic 1970
Ogeechee River	H13	Closed-end	Steel	Circular	8.9	0.457	2497	2578	5.99	0.79	Vesic 1970
Ogeechee River	H14	Closed-end	Steel	Circular	12.0	0.457	2700	3318	5.23	0.75	Vesic 1970
Ogeechee River	H15	Closed-end	Steel	Circular	15.0	0.457	3116	3624	5.31	0.73	Vesic 1970
Pidgeon Creek	1	Closed-end	Steel	Circular	6.9	0.356	1212	1617	4.26	0.67	Paik et al. 2003
Sermide	S	Closed-end	Steel	Circular	35.9	0.508	4408	4998	9.13	0.66	Appendino 1981

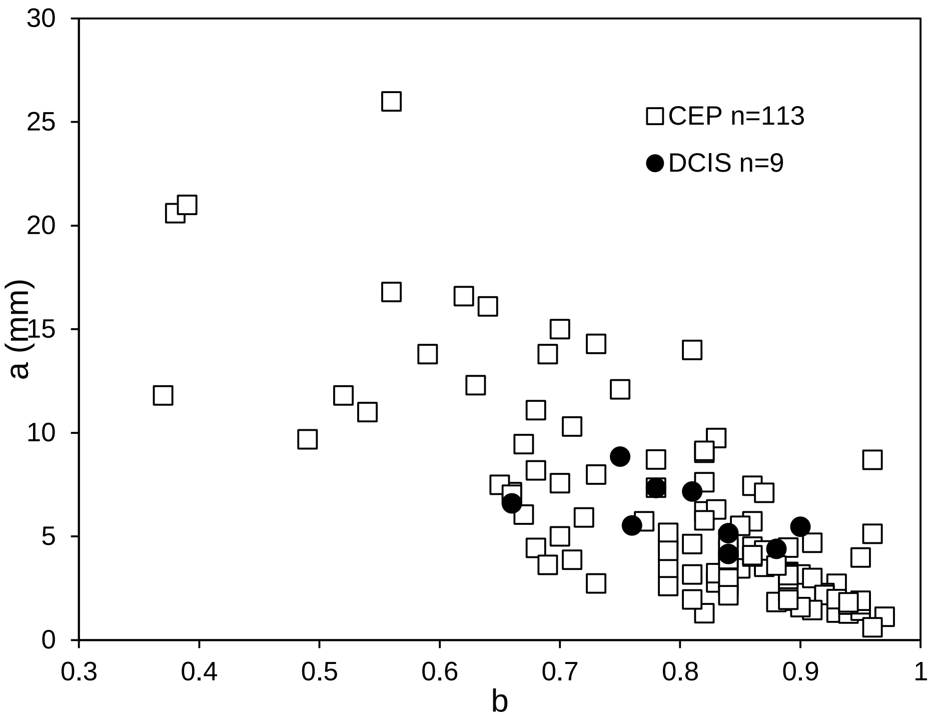

Fig. D1. Scatter plot of hyperbolic parameters for DCIS and closed-ended piles, reported by Tang & Phoon (2018)

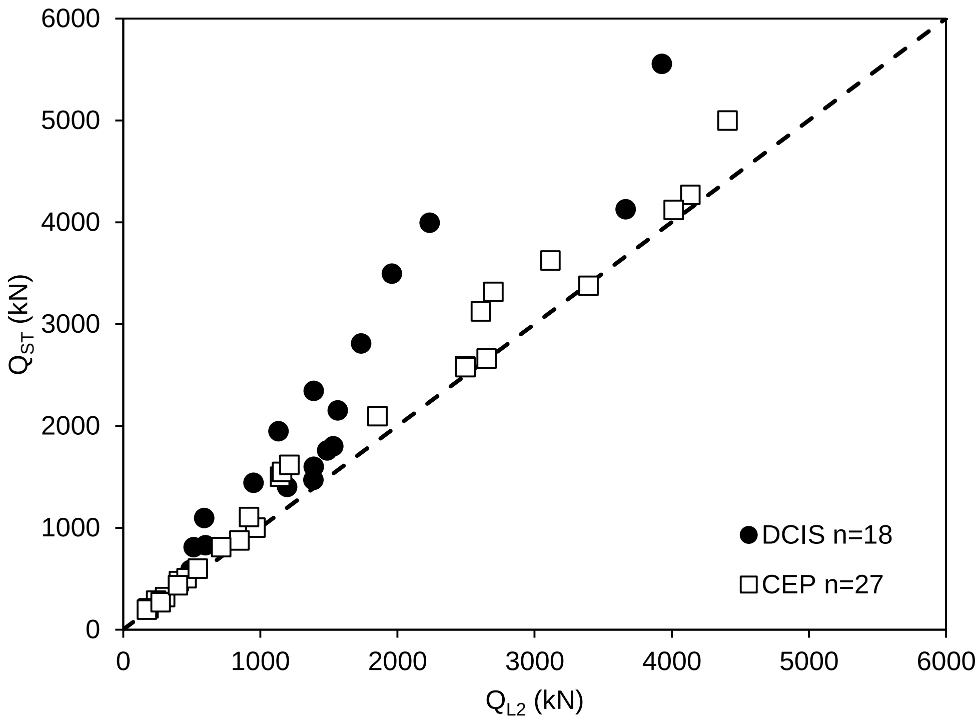

Fig. D2. Comparison of interpreted loads for DCIS and closed-ended piles

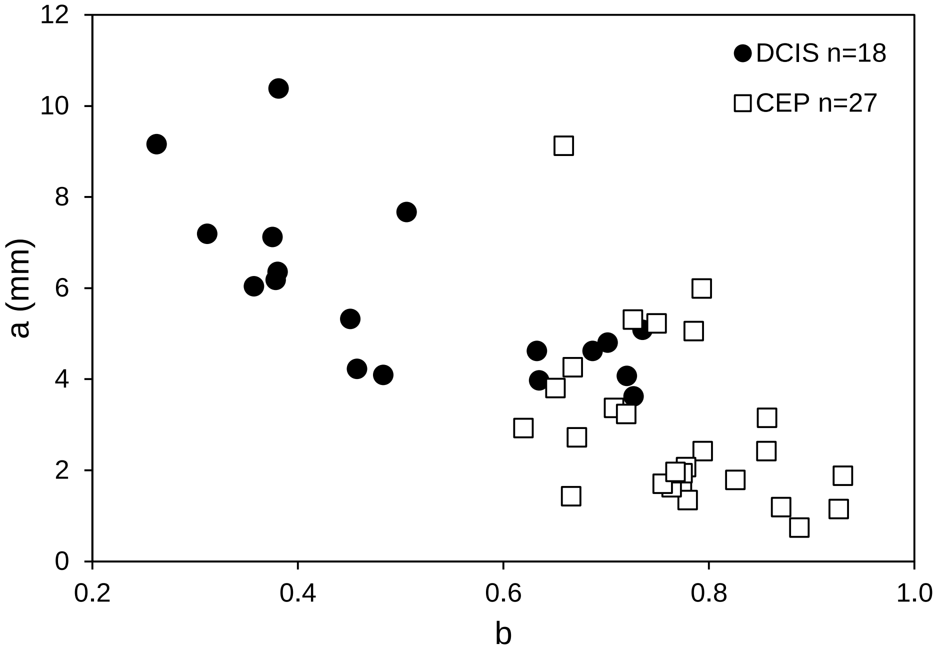

Fig. D3. Scatter plot of hyperbolic parameters for DCIS and closed-ended piles interpreted using the slope tangent resistance